

# Dissociation-ionization and ionization-dissociation by multiphoton absorption of acetaldehyde at 266 and 355 nm. Dissociation pathways

J.C. Poveda<sup>a</sup>, I. Álvarez<sup>b</sup>, A. Guerrero-Tapia<sup>b</sup>, and C. Cisneros<sup>b</sup>

<sup>a</sup>Laboratorio de Espectroscopia Atómica Molecular,

Escuela de Química-Facultad de Ciencias-Universidad Industrial de Santander, Bucaramanga Santander-Colombia A.A. 678.

e-mail: jcpoveda@uis.edu.co; jkclim@fis.unam.mx

<sup>b</sup>Laboratorio de Colisiones Atómicas, Moleculares y Óptica Experimental,

Instituto de Ciencias Físicas-Universidad Nacional Autónoma de México, Cuernavaca-Morelos México, 62210.

Received 18 September 2015; accepted 12 January 2016

The experimental results from the interaction of a sample of acetaldehyde ( $\text{CH}_3\text{CHO}$ ) with laser radiation at intensities between  $10^9$  and  $10^{11}$   $\text{Wcm}^{-2}$  and wavelengths of 266 and 355 nm are reported. As a result of multiple photon absorption, cations from ionization-dissociation (I-D) or dissociation-ionization (D-I) processes, were detected using a reflectron time of flight mass spectrometer. The processes I-D is predominant at 355 nm and D-I is predominant at 266 nm. The formation of different ions is discussed. From analysis of the ratios between the ion currents  $[\text{I}(\text{CH}_3\text{CO}^+) + \text{I}(\text{CO}^+) / [\text{I}(\text{CH}_3^+) + \text{I}(\text{HCO}^+) ]$ , originated from the C-C bond or from the C-H bond breaking at different laser intensities, the predominant channels are determined.

**Keywords:** Acetaldehyde; photoionization; photodissociation; multiphoton processes; molecular dissociation.

PACS: 32.80.Rm; 32.80.Wr; 33.15.Ta

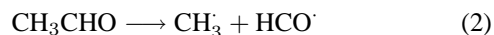
## 1. Introduction

Different sources contribute to the formation of acetaldehyde: anthropogenic, plants, biomass burning, surface of the oceans, being its largest source, the oxidation of hydrocarbons. Photochemistry of acetaldehyde had been previously analyzed; it can be decomposed by photolysis [1]. The interaction of acetaldehyde with the radical  $\text{HO}^\cdot$  allows the hydrogen abstraction to produce the acetyl radical, and with ions and radicals such as  $\text{HO}^\cdot$  and  $\text{NO}_2$  produces peroxyacetyl nitrate ( $\text{CH}_3\text{C}(\text{O})\text{O}_2\text{NO}_2$ ). Acetaldehyde has been detected during combustion processes as a part of radical reactions [2], is sensible to oxidation processes, resulting in the formation of acetic acid [3]. It also has been studied using different experimental and theoretical methods [4-9]. The electronic, rotational and vibrational structure has been reported [10-14]. Electronic energy levels and associated vibrational progressions have been measured using various techniques [15,16]. Due to the fact that acetaldehyde is a small molecule, the analysis of experimental data can be accomplished comparing them with quantum chemical calculations [15-18]. Previous results show that when the acetaldehyde molecule absorbs photons in the UV wavelength range, between 250 and 350 nm [19] the transition  $S_0 \rightarrow S_1$  occurs through a  $n \rightarrow \pi^*$  states and it dissociates through various channels that lead to different neutral products. In condensed and gas phases vinyl alcohol can be formed by intermolecular proton transfer keto-enol equilibrium process [20-23]:



The energies of the first excited electronic states of acetaldehyde are shown in Table I.

The accessible dissociation channels by absorption of a single photon at wavelengths below 318 nm (3.89 eV) are:



The channel (2) is possible through the  $T_1$  state by an inter-system crossing process (ISC) with the  $S_1$  state [24,1]. The radicals  $\text{CH}_3$  and  $\text{HCO}^\cdot$  can result from the dissociation of the acetyl radical after hydrogen abstraction [25,26]. In the  $S_1$  state, the acetaldehyde can dissociate to form hydrogen and the  $\text{CH}_3\text{CO}^\cdot$  radical in an excited state, following the channel (3). Furthermore, as it has been reported [27],  $\text{CH}_4$  and  $\text{CO}$  must arise from the non-degenerate singlet ground state  $S_0$ , channel (4),



Other important channel is the hydrogen elimination channel (5):



The channels (3) and (5) are also a result of an ISC mechanism, between the  $S_1$  and  $T_1$  [28].

The molecular products  $\text{CH}_4$  and  $\text{CO}$  are obtained through channel (4) at wavelengths shorter than 248 nm, while the hydrogen atom elimination channels (3) and (5) emerge from the photodissociation of acetaldehyde at 205 nm [17]. Channel (3) dominates over channel (5) due to the different transition energy values: 24.4 and 42.5 kcal/mol. Other reported channel [29], which leads to hydrogen neutral molecule elimination, is:

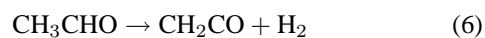


TABLE I. Excitation energies of acetaldehyde.

	Excitation energies, eV					
	Calculated			Observed		
	Authors <sup>a</sup>	Wiberg <sup>b</sup>	Gwaltney <sup>c</sup>	Robin	Kim	Limão-Vieira
<b>(a) Singlets:</b>						
Functional	B3LYP	B3P86	B3P86			
1A'' ( $n \rightarrow \pi^*$ )	4.357	4.354	4.29	4.32	4.28	3.69
1A'	6.198	6.470	6.76	6.79	6.82	6.82
1A'	6.758	7.007	7.29	7.47	7.46	7.456
1A''	7.120	7.388	7.70	7.75		7.73
1A'	7.336	7.643	7.89	7.80	7.75	
1A'	7.883	8.114	8.35	8.54	8.43	8.434
1A'	8.271	8.557	8.76	8.75	8.69	8.628
1A''	8.626	8.618	9.30	8.90		
<b>(b) Triplets:</b>						
3A'' ( $n \rightarrow \pi^*$ )	3.729	3.618	3.65			3.679
3A' ( $n \rightarrow \pi^*$ )	6.015	5.950	5.72			
3A'	6.067	6.317	6.58			
3A'	6.648	6.874	7.16			
3A''	7.107	7.365	7.67			
3A'	7.28	7.593	7.89			

<sup>a</sup>Time-Dependent Density Functional Theory, Functional B3LYP and B3P86, 6-311++G(3df,3pd) basis set.

<sup>b</sup>Time-Dependent Density Functional Theory, Functional B3P86, 6-311++G(d, p) basis set.

<sup>c</sup>Equation-of-Motion Coupled Clusters Method, [5s3d2d/3s2p] basis set.

All of the above processes, channels (2) to (6) can take place in one photon absorption regimes and the resulting neutral products have been reported. For instance the absorption of one-photon of 266 nm allows the neutral molecule reach the  $S_1$  state. If there is not an excess of energy transferred during the excitation, the  $S_1$  state can decay to  $S_0$  by an internal conversion processes IC, and form other products [29,30], including  $\text{CH}_4$  and CO.

In the present work, the photodissociation and photoionization of acetaldehyde in the multiple photon absorption regimes were investigated at wavelengths of 266 and 355 nm and intensities of radiation in the range  $10^8$  to  $10^{11}$   $\text{W}\cdot\text{cm}^{-2}$ . Radiation interacts with a cooled molecular beam of acetaldehyde produced by the adiabatic expansion of vapors into a high vacuum chamber at  $10^{-8}$  torr. The resulting ions were analyzed using a home-assembled Jordan R-TOF mass analyzer.

On the basis of the detected ions at 266 and 355 nm, the processes were identified as D-I and I-D, respectively. The number of photons required to form a particular ion was calculated accordingly with the Keldysh approximation [31] and compared with the reported electronic energy levels [32,8]. Along with those, based on the detected ions, the different dissociation pathways were proposed.

This work gives new insights on the molecular physical processes present when acetaldehyde molecules interact with

photons and the products that can emerge as result of photoionization and photodissociation.

## 2. Experimental

The photoionization and photodissociation of acetaldehyde was analyzed using the experimental setup previously described [33]. Briefly, a sample of acetaldehyde (99%), purchased from Sigma Aldrich Chemical Corp) was used as received. The sample was connected to a pulsed injection valve, IOTA-ONE. A cooled molecular beam of acetaldehyde, with helium as a carrier gas was produced by adiabatic expansion in a high-vacuum chamber at  $2 \times 10^{-8}$  torr. The pulsed valve was synchronously coupled with the laser pulses with an opening time of 250  $\mu\text{s}$  to achieve an operating pressure of  $2 \times 10^{-6}$  torr. The 355 nm laser radiation was produced from the third harmonic of a Nd:YAG laser, operating at 30 Hz repetition rate (Spectra Physics). The laser pulse width is 5.5 ns and the energies per pulse from 1 to 30 mJ. When it was required, 266 nm photons were produced from the fourth harmonic by pumping a second crystal, frequency doubler, with 532 nm pulses of radiation. Thus, 266 nm photons with pulse widths of 3.5 ns and energies per pulse from 0.1 to 10 mJ were used. The laser radiation (with a Gaussian profile and linearly polarized) was focused into the interaction region using a 15 cm focal length lens. The diameter

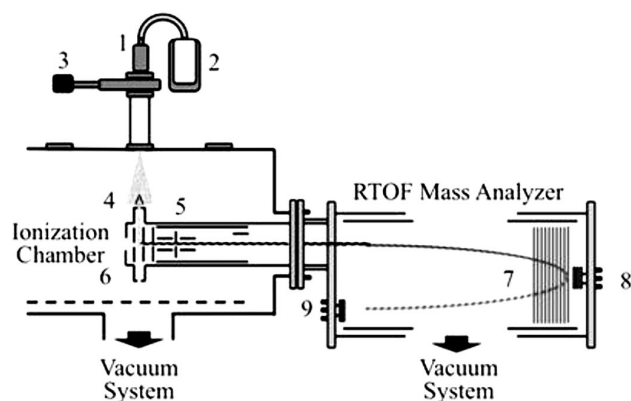


FIGURA 1. Experimental setup. 1. Pulsed valve, 2. Sample reservoir, 3. Valve, 4. Skimmer, 5. Electrostatic lenses, 6. Extraction and acceleration plates, 7. RTOF Electrostatic lenses, 8, 9 Detectors.

at the focal point was  $80.0 \mu\text{m}$ . Under these experimental conditions, radiation intensities between  $10^9$  and  $10^{11} \text{ W}\cdot\text{cm}^{-2}$  were achieved. The cooled molecular beam interacted orthogonally with the laser radiation at a point located between two parallel plates continuously polarized at 5.0 and 4.5 keV, corresponding to the extraction and the acceleration potentials, respectively. The distance between the plates was 0.8 cm. Holes of 10 mm diameter at the center of each plate with a fine metal mesh were used to extract the positively charged ions from the interaction region. The ions were driven along the field-free region of the reflector R-TOF analyzer and eventually reached a double microchannel detector after they were refocused; Figure 1 shows the experimental setup. The ions arrived to the detector, according to their masses. The resolution archived was of the order of 3000. The current signal was pre-amplified, voltage-converted, digitized and sampled in time using an EG&G Ortec multichannel analyzer. The resulting detector signal after each laser pulse was processed using a temporal window of  $50 \mu\text{s}$  and 80000 channels at 0.625 ns per channel. Signals from 5000 laser shots were added to obtain the final spectra. Spectra were obtained at different energies per pulse in the intervals from 0.1 to 10.0 mJ at 266 nm and 1.0 to 20.0 mJ at 355 nm.

### 3. Results and Discussion

The ions from PI and PD process were characterized by R-TOF mass spectrometry technique. The spectra were measured at different energies per pulse. Each ion current was analyzed as it changes as a function of the energy per pulse. When the photon density increases, new ions can be formed, and the TOF mass spectra changes, see Figs. 2 and 3. If two photons of 266 nm (9.32 eV) are absorbed, it results in the dissociation of the molecule along the C(O)-H coordinate to form the  $\text{CH}_3\text{CO}^+$ , represented as channel (3), and the ions are formed later. The photophysical processes are mainly dissociation-ionization since only very low current of the parent ion was detected. The acetyl radical absorbs pho-

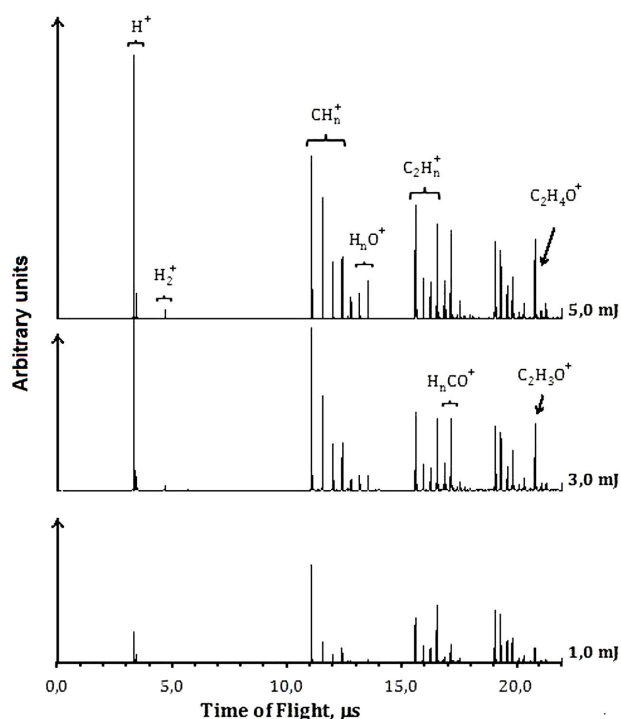


FIGURA 2. TOF spectra of acetaldehyde at 266 nm.

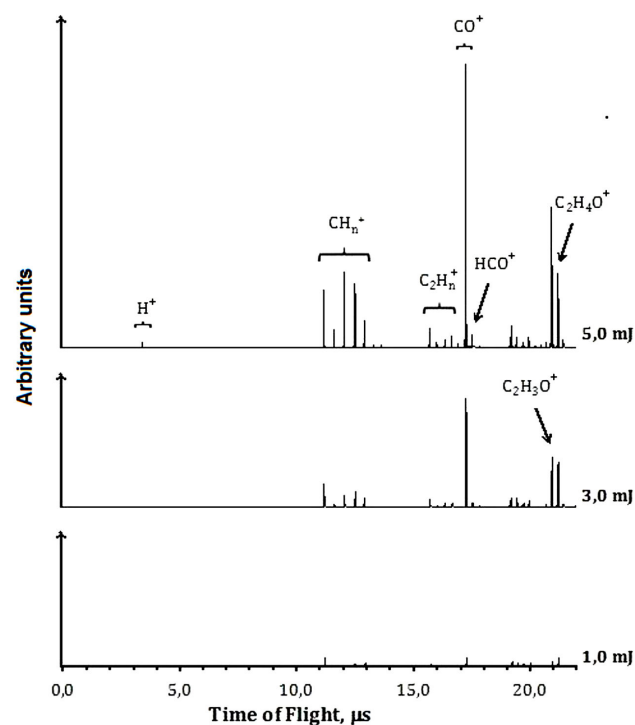


FIGURA 3. TOF spectra of acetaldehyde at 355 nm.

tons and gets ionized and dissociated Fig. 2. The main ions detected in the TOF mass spectra correspond to  $\text{CH}_3\text{CO}^+$  (43),  $\text{HCO}^+$  (29),  $\text{CO}^+$  (28),  $\text{CH}_3^+$  (15),  $\text{CH}_2^+$  (14),  $\text{CH}^+$  (13),  $\text{C}^+$  (12), and  $\text{H}^+$  (1). Minor quantities of  $\text{H}_2\text{O}^+$  (18),  $\text{HO}^+$  (17), and  $\text{H}_2^+$  (2) were also observed. The ions  $\text{C}_2\text{H}_3^+$  (27),  $\text{C}_2\text{H}_2^+$  (26),  $\text{C}_2\text{H}^+$  (25), and  $\text{C}_2^+$  (24) were also present

they can be interpreted by the possible presence of the tautomer vinyl alcohol that leads to the formation of such ions. Additionally, we observe CH<sub>3</sub>CHOH which can be produced from dimmers of acetaldehyde present in the original sample.

At 355 nm and low energies per pulse, such as 1.0 mJ, the molecular ionization or dissociation processes are poorly observed. Increasing the energies, as to 3.0 mJ per pulse, the presence of the molecular parent ion, CH<sub>3</sub>CHO<sup>+</sup>, the acetyl cation, CH<sub>3</sub>CO<sup>+</sup>, and CO<sup>+</sup>, are evident, Fig. 3. As the energy per pulse increases, around 5.0 mJ, the cations: C<sup>+</sup>, CH<sup>+</sup>, CH<sub>2</sub><sup>+</sup>, CH<sub>3</sub><sup>+</sup> and CH<sub>4</sub><sup>+</sup> were also observed.

The presence of CH<sub>4</sub><sup>+</sup> is a signature of intermolecular hydrogen transposition, which takes place due to the C-C bond breaking via the roaming mechanism, channel (7), as it has been previously reported [29].



Hydrogen cleavage to produce H<sup>+</sup> is a non-favored channel; H<sup>+</sup> is detected only in very low quantities. Contrary to the case at 266 nm, the ions resulting from vinyl alcohol dissociation were not present.

### 3.1. Energies of the Processes

For multiple-photon absorption, the number of photons and from them the energy for the formation of a particular ion via ionization or dissociation processes can be calculated using the ion currents measured as a function of the radiation intensity, applying the Keldysh relation,  $Y = A \cdot I^n$  [31]. Where,  $Y$  is the ion yield of a particular ion,  $I$  is the intensity of radiation in  $\text{W} \cdot \text{cm}^{-2}$ ,  $n$

is the number of photons for the formation of the ion, and  $A$  is a function of the  $n$ th order cross section. At low energies per pulse when the process follows the Keldysh's relation, the value  $n$  can be readily calculated. As the radiation intensity increases, it is possible to reach the saturation limit, and the calculated values of  $n$  decrease. Calculated  $n$  values and the equivalent energy for the main detected ions of acetaldehyde at 266 nm and 355 nm are shown in Table II along with their ionization energies, previously reported [34].

Most of the energies calculated from the number of photons leading to a particular ion are in good agreement with the reported values. In some cases, the number of photons  $n$  gives the energy to form a particular ion coming from the neutral acetaldehyde or from the acetyl radical produced after the acetaldehyde dissociation, Table II.

### 3.2. Dissociation-Ionization at 266 nm

Accordingly to Table I the absorption of two 266 nm photons allows the neutral acetaldehyde molecule access different electronic states. The energy of one photon exceeds the  $S_1$  state, but it is not enough to reach the  $S_2$  state, however, at high photon densities such as in the present experiments, two-photon absorption is possible. The two photon supply an energy of 9.32 eV and electronic transitions to molecular

TABLE II. Calculated energy values, in eV, from the number of photons absorbed using the Keldysh approach [31].

Ion	Wavelength, nm		Ionization Energy*, eV
	266	355	
H <sup>+</sup>	14.39	—	13.60
CH <sup>+</sup>	—	13.75	10.64
CH <sub>2</sub> <sup>+</sup>	—	14.31	10.40
CH <sub>3</sub> <sup>+</sup>	9.78	14.27	9.84
CH <sub>4</sub> <sup>+</sup>	9.69	13.99	12.61
OH <sup>+</sup>	13.74	—	13.02
H <sub>2</sub> O <sup>+</sup>	10.15	—	12.65
C <sub>2</sub> H <sub>3</sub> <sup>+</sup>	13.69	—	8.25
CO <sup>+</sup>	9.73	13.61	14.01
CHO <sup>+</sup>	8.57	10.61	8.12
CH <sub>3</sub> CO <sup>+</sup>	9.41	10.53	8.03
CH <sub>3</sub> CHO <sup>+</sup>	—	9.87	10.23

\*From reference [37].

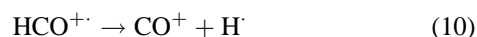
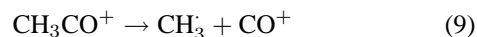
Rydberg states occur. The excited molecule can decay to the triplet state  $T_2$ , along the channels CH<sub>3</sub>CO-H or CH<sub>2</sub>-CHO. But, if the photon density increases the three-photon absorption is possible and acetaldehyde molecules are ionized. At 266 nm and intensities of radiation of  $10^9$  to  $10^{11} \text{ W} \cdot \text{cm}^{-2}$ , the dominant process is the dissociation-ionization; the molecular parent ion was poorly observed.

The formation of C<sub>2</sub>H<sub>3</sub>O<sup>+</sup> is possible by three different dissociation mechanisms; two of them arising from the neutral molecule dissociation, channels (3) and (5), followed by ionization, making two the number of photons needed for the ionization of neutral CH<sub>3</sub>CO<sup>+</sup>, see Table II. Another channel that leads to the formation of CH<sub>3</sub>CO<sup>+</sup> is the direct neutral hydrogen elimination from the molecular parent ion, channel:



The formation of the radical HCO<sup>+</sup> at 266 nm, only takes place by one mechanism, the molecular dissociation channel (2), followed by ionization. The energy calculated from the number of absorbed photons leading to the ionization of HCO<sup>+</sup> at 266 nm is in good agreement with the reported ionization potential of 8.12 eV [37], see Table II.

CO<sup>+</sup> arises from two different mechanisms, by dissociation of acetyl cation, channel (9), and from dissociation of HCO radical cation, follow by ionization, channel (10).



Finally, the formation of H<sup>+</sup> results also from two different processes, single dissociation: C-H, bond breaking, from

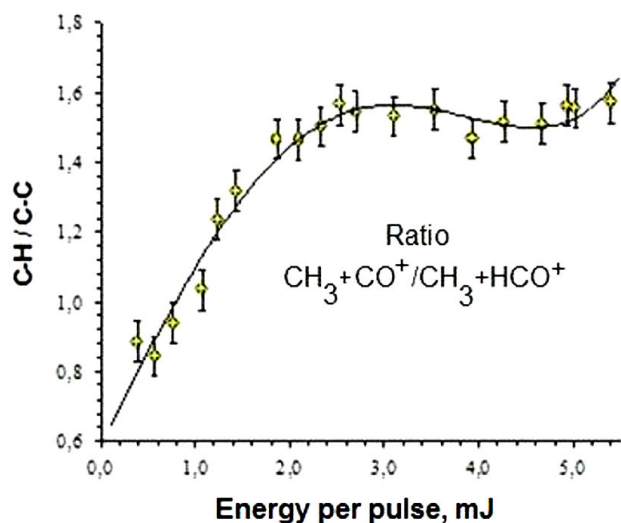


FIGURA 4. Ratio of ion yield of the two main radical channels in the Photodissociation of acetaldehyde at 266 nm.

cations such as  $\text{CH}_3\text{CO}^+$ , channel (11), and  $\text{HCO}^+$ , channels (12), Fig. 2.



For the main dissociation channels, the C-C bond dissociation that produces  $\text{CH}_3$  and  $\text{HCO}^{\cdot}$  radicals requires an energy near 4.15 eV, while the C-H bond dissociation that produces  $\text{CH}_3\text{CO}^{\cdot}$  and  $\text{H}^{\cdot}$ , requires 3.85 eV [28].

Figure 4 shows the ratio of ion currents  $\text{CH}_3\text{CO}^+ + \text{H}^+ / \text{CH}_3 + \text{HCO}^+$  calculated from the integrated signals obtained from the TOF spectra. Below 2 mJ the ratio increases, indicating that processes:  $\text{CH}_3\text{CO} + \text{H}$  is the most favored.

### 3.3. Ionization-Dissociation at 355 nm

At 355 nm, based on the detected ions, we can propose a mechanism for the formation of ions identified in the TOF spectra, see Fig. 3. The absorption of one 355 nm photon (3.493 eV) does not supply enough energy to reach the first excited state  $S_1$  (4.29 eV,  $n \rightarrow \pi^*$  transition) [35]. The absorption of two photon supplies sufficient energy to reach the  $S_2$  electronic state (originally at 6.822 eV,  $n \rightarrow 3s$ ) Rydberg transition [5,36,12,6] see Table I. If from this state the molecule absorbs one more photon, then it can be ionized, confirm that the ionization takes place by a [2+1] resonant absorption, via the  $\nu_5$  ( $5_0^1$ ) vibrational state of the  $S_2$  state [12,16,36,38]. Since three photons yield energy of 10.479 eV, it is enough to ionize the neutral molecule. From the molecular parent ion, various dissociation channels are proposed to explain the TOF spectra, based on the absorbed energy (number of photons) as follows:

Three photon channels:

Hydrogen elimination:



C-C bond dissociation:

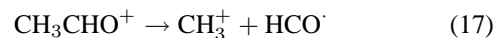


Four photon channels:

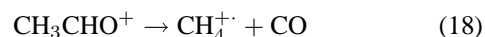
Hydrogen elimination:



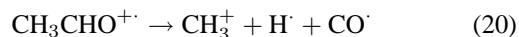
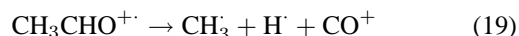
C-C bond dissociation:



Hydrogen transposition via the roaming mechanism:



Double bond dissociation:



We suggest that the formation of the  $\text{CO}^+$  cation could be produced through channel (19) or by the dissociation of  $\text{HCO}^+$ , channel (16). Channel (20) contributes to increase the ion current of  $\text{CH}_3^+$ , also obtained following the channel (17).

If  $\text{CO}^+$  formation proceeded by the dissociation of  $\text{HCO}^+$  ions through channel (16), we would expect higher ion currents of  $\text{HCO}^+$  for low-density photons, but this was not the case. Then the probability that  $\text{CO}^+$  is formed through channel (19) is the highest.

From a theoretical point of view, the C-H channel dominates over the C-C channel when the molecular parent ion dissociates. Experimentally, the ion yields of  $\text{CH}_3\text{CO}^+$  were higher than those of  $\text{CH}_3^+$  at the energy per pulse intervals used in our experiments. As it was pointed out the absorption of three 355 nm photons (10.47 eV) yields sufficient energy for molecular ionization (10.23 eV), and an excess of energy is available, enabling the C-H dissociation. Whereas the C-C bond dissociation requires higher energies such as those that should be supplied by the absorption of four photons (13.76 eV).

### 3.4. Intramolecular hydrogen transposition

At 266 nm, the spectra were characterized by the appearance of fragment ions different from those obtained by the direct DI process of acetaldehyde. Such ions are the result of the dissociation of the ionized vinyl alcohol. The ratio of the ion currents resulting from the dissociation of vinyl alcohol and acetaldehyde ( $\sum I_{\text{CH}_2=\text{CHOH}} / \sum I_{\text{CH}_3\text{C(O)H}}$ ) was calculated at the energies per pulse used in our experiments, and the results are presented in Fig. 5. For energies per pulse < 1 mJ, the ions coming from vinyl alcohol were present. However, as the energy per pulse increases, the acetaldehyde

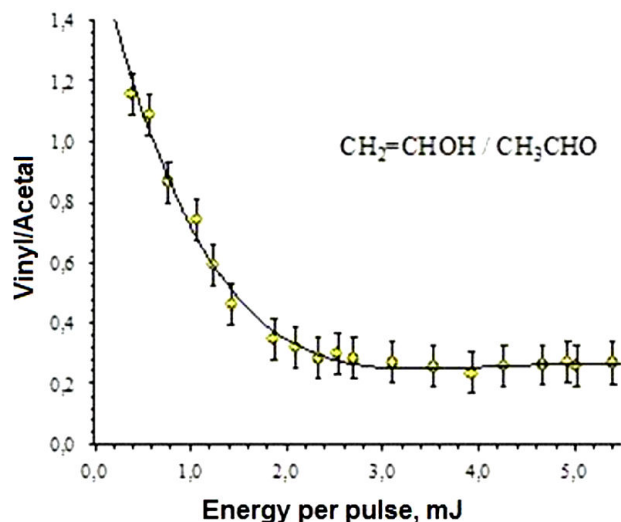


FIGURA 5. Ratio of ion yields of vinyl channels to acetaldehyde channels at 266 nm.

dominates, that is possible because the acetaldehyde molecular dissociation is faster than hydrogen intramolecular transposition, as the energy per pulse increases the signals from dissociation-ionization of vinyl alcohol are only a small fraction of the total ion current.

As it was previously mentioned, the energy barriers for enolization were calculated for the neutral and cation forms of acetaldehyde. In the neutral form, the energy barrier (3.00 eV) is higher than that calculated in the cation (2.71 eV) by approximately 0.29 eV [21,12]. In the cation, the equilibrium is displaced to the enol (vinyl alcohol) because the alcohol has a lower energy than acetaldehyde, with an energy difference of about 0.48 eV. These results are in agreement with of ion yields at lower energies per pulse, see Fig. 5.

At 355 nm there is a resonant process, the neutral molecule is ionized, however only their daughter ions were observed in the TOF spectra, see Fig. 3. Excess of energy allows the equilibrium to the formation of vinyl alcohol cation, their daughter ions were observed, but not as efficiently as it occurs at 266 nm.

#### 4. Conclusions

Multiphoton I-D D-I studies are an excellent tool to address the main process that take place when photons interact with neutral species. In the present work, it is reported the analysis of photoionization and photodissociation of acetaldehyde using laser radiation of 266 nm and 355 nm in a cooled molecular beam. TOF-MS spectra are presented. At 266 nm, photon absorption is followed by a D-I mechanism, while at 355 nm, the I-D mechanism occurs. Some new dissociation channels were proposed based on cations detected from the I-D or DI processes.

At 266 nm, the spectra show a signal attributed to the dissociation-ionization of vinyl alcohol, which arises from the gas phase molecular equilibrium of the acetaldehyde transformed into to vinyl alcohol. For the case of 355 nm a quasi-resonant processes is observed and there are several differences with the 266 nm spectra.

#### Acknowledgments

This work was financial supported by the projects PAPIIT-UNAM, IN101215 and IN102613 and CONACyT, grant 165410. Author J.C. Poveda thanks the support of Vicerectoría de Investigaciones y Extensión of the Universidad Industrial de Santander.

1. P. Warneck and G.K. Moortgat, *Atmos. Environ.* **62** (2012) 153.
2. A. Arnold *et al.*, *Opt. Lett.* **15** (1990) 831.
3. M. Bowker and R.J. Madix, *Appl. of Surf. Sci.* **8** (1981) 299.
4. N.C. Shand, Ch. L. Ning, M.R.F. Siggel, I.C. Walker, and J. Pfab, *J. Chem. Soc. Faraday Trans.* **93** (1997) 2883.
5. N.C. Shand, C.L. Ning, and J. Pfab, *Chem. Phys. Lett.* **247** (1995) 32.
6. H.T. Kim, and S.L. Anderson, *J. Chem. Phys.* **114** (2001) 3018.
7. P.L. Houston and S.H. Kable, *Proc. Nat. Acad. Sci.* **103** (2006) 16079.
8. B. A. Heath, M.B. Robin, N.A. Kuebler, G.J. Fisanick and T.S. Eichelberger, *J. Chem. Phys.* **72** (1980) 5565.
9. G.J. Fisanick, T.S. Eichelberger, *J. Chem. Phys.* **74** (1981) 6692.
10. E. Jalviste, G. Berden, M. Drabbles and A.M. Wodtke, *J. Chem. Phys.* **114** (2001) 8316.
11. S.H. Jen, T. J. Hsu and I. Ch. Chen, *Chem. Phys.* **232** (1998) 131.
12. Y. Kim, J. Fleniken, and H. Meyer, *J. Chem. Phys.* **109** (1998) 3401.
13. T. Kono, M. Takayanagi, and I. Hanazaki, *Laser Chem.* **15** (1995) 249.
14. M.A. Buntine, G.F. Metha, D.C. Mcgilvery, and R.J.S. Morrison, *J. Mol. Spectrosc.* **165** (1994) 12.
15. Y. Kim and H. Meyer, *Chem. Phys. Lett.* **387** (2004) 339.
16. P. Limão-Vieira, S. Eden, N.J. Mason, and S.V. Hoffman, *Chem. Phys. Lett.* **376** (2003) 737.
17. Y. Kurozaki, *J. Mol. Struct. THEOCHEM* **850** (2008) 9.
18. S.R. Gwaltney, and R.J. Bartlett, *Chem. Phys. Lett.* **241** (1995) 26.
19. S.P. Sander, D.M. Golden, M.J. Kurylo, G.K. Moortgat, and P.H. Wine, *Chemical Kinetics and Photochemical Data for Use in Atmospheric Studies*, Evaluation Number 15, JPL Publication 06-2, (2006).

20. L. Rodríguez-Santiago, O. Vendrell, I. Tejero, M. Sodupe, and J. Bertran, *Chem. Phys. Lett.* **334** (2001) 112.
21. G. van der Rest, H. Nedev, J. Chamot-Rooke, P. Mourgues, T. B. McMahon, and H.E. Audier, *Int. J. Mass Spec.* **202** (2000) 161.
22. R.J. Payne, M.J.T. Jordan, and Sc.H. Kable, *Science* **337** (2012) 1203.
23. G. da Silva, and J.W. Bozzelli, *Chem. Phys. Lett.* **483** (2009) 25.
24. N.M. Cordeiro, E. Martínez-Núñez, A. Fernández-Ramos, and S.A. Vázquez, *Chem. Phys. Lett.* **375** (2003) 591.
25. Y. Kurosaki, *Chem. Phys. Lett.* **421** (2006) 549.
26. Y. Kurosaki, and K. Yokohama, *Chem. Phys. Lett.* **371** (2003) 568.
27. B. Gherman, R.A. Friesner, T. H. Wong, Z. Min, and R. Bersohn, *J. Chem. Phys.* **114** (2001) 6128.
28. T.Y. Kang, S.W. Kang, and H.L. Kim, *Chem. Phys. Lett.* **434** (2007) 6.
29. L. Rubio-Lago, G.A. Amaral, A. Arregui, J. González-Vázquez, and L. Bañares, *Phys. Chem. Chem. Phys.* **14** (2012) 6067.
30. B.R. Heazlewood *et al.*, *Proc. Nat. Acad. Sci.* **105** (2008) 12719.
31. L.V. Keldysh, *Sov. Phys. JETP* **20** (1965) 1307.
32. V. A. Shubert, and S.T. Pratt, *J. Phys. Chem. A.* **114** (2010) 11238.
33. J.C. Poveda, A. Guerrero, I. Álvarez, and C. Cisneros, *J. Photochem. Photobiol. A: Chem.* **215** (2010) 140.
34. J.D. Coffman, M. Gallmann, and I.V. Hertel, *Z. Physik D.* **12** (1989) 297.
35. K.B. Wiberg, R.E. Stratmann, and M.J. Frisch, *Chem. Phys. Lett.* **297** (1998) 60.
36. J.G. Philis and C. Kosmidis, *J. Mol. Struct.* **99** (2001) 563.
37. *NIST Standard Reference Data Program*, National Institute of Standards and Technology (2014)
38. K.N. Walzl, C.F. Koerting, and A. Kuppermann, *J. Chem. Phys.* **87** (1987) 3796.